Discovery of FS36 as a Novel Human Hsp90 Inhibitor*

LI Gen[1], LÜ Kai-Kai[2], LI Jian[1, 3], YIN Xiu-Shan[1, 4], ZHAO Dong[5], ZHANG Wan-Zhong[1]**

([1] *College of Pharmaceutical and Biological Engineering, Shenyang University of Chemical Technology, Shenyang* 110142, China;
[2] *Shanghai Institute of Materia , University of Chinese Academy of Sciences, Shanghai* 201203, China;
[3] *Department of Molecular & Cellular Biochemistry, College of Medicine, University of Kentucky, Lexington*, KY 40536, USA;
[4] *Karolinska Institutet* (*MTC*), *Science for Life Laboratory, Tomtebodavāg, en 23A* (*Gamma5*), 17165 Solna, Sweden;
[5] *Shaanxi Key Laboratory of Ischemic Cardiovascular Disease; Institute of Basic & Translational Medicine,*
Xi' an Medical University, Xi' an 710021, China)

Abstract The heat shock protein 90 (Hsp90) plays an important role in growth and progression of tumor cells through the appropriate folding, conformational maturation and activation of several hundred protein substrates (client proteins). Thus, Hsp90 attracts a great many of interests as a promising target for antitumor drugs which results in more than 20 inhibitors advancing to clinical trials. Here, we designed and synthesized a small molecule inhibitor: FS36 and the X-ray diffraction data of the complex crystal of Hsp90^N-FS36 is collected. High-resolution X-ray crystallography shows that FS36 interacts with Hsp90^N at the ATP-binding pocket and this demonstrates that FS36 possibly substitutes nucleotides to bind to Hsp90^N. The complex crystal structure and the interactions between FS36 and Hsp90^N lay the foundation of the design and majorization of novel antitumor drugs.

1 Introduction

X-ray diffraction (XRD) is a non-destructive analytical technique which reveals information about the protein crystal structure, chemical composition and physical properties of materials. Nowadays, XRD is a conventional method for determining how small molecule inhibitors interact with their targets and how to improve the compounds based on complex crystal structures of ligand-targets. It provides an exhaustive interaction of the protein-compound for drug design and structural modification, thus becoming the main technology in the field of drug discovery and providing a rational basis for designing more effective and safer drugs[1-3].

The heat shock protein 90 (Hsp90) functions as α-α or β-β homodimer and the dimerization is necessary for the maintenance of its functions *in vivo*[4].

An Hsp90 monomer is composed of three highly conserved domains: an N-terminal domain, which mediates the binding of ATP/ADP[5]; a middle domain, which plays a significant role in ATP hydrolysis and owns a large hydrophobic surface to combine the client proteins to further their folding; and a C-terminal domain which is responsible for dimerization of Hsp90[6]. The first crystal structure of N-terminus of human Hsp90 (Hsp90^N), discovered by Stebbins *et al*. [7] demonstrates an α/β sandwich with a 15Å deep pocket

whose diameter for entrance is 12Å and for base is 8Å. Eight continuous anti-parallel β sheets constitute the base, while the wall is made up of three α helices and a loop (H2-H4-H7-L1). The hydrophobicity of the pocket increases from the entrance to the base[8–12].

Hsp90 is a highly conserved molecular chaperone that is characterized by elevated gene expression during stress conditions[13]. Dual chaperone functions of Hsp90 exist. One is participating in maintaining protein homeostasis by the proper folding or refolding and activation of several hundred client proteins in the cell, the other is taking part in the cellular stress response[14]. With more than 300 known client proteins which participate in signal transduction and assembly, it has been considered to be a potential target for diseases associated with many abnormal protein signals such as cancer, infectious and neurodegenerative diseases[15–18].

Inhibitors targeting the ATP binding pocket of the N-terminal domain have been well-studied, many of which have been put into clinical trials. The first Hsp90 inhibitor: geldanamycin (GDM) and another significant natural inhibitor: radicicol reveal effective antiproliferative activity by binding to the ATP binding pocket[17]. The mechanism of GDM as an antitumor antibiotic preclinical research was obscure until the crystal structure of Hsp90^N-GDM complex was confirmed. It manifests that the way GDM works by blocking the binding of ATP to Hsp90 makes the conformational rearrangement of Hsp90 failed, resulting in Hsp90 unable to promote conformational maturation, stability and activation of client proteins. Radicicol works in a semblable way[19–20]. Followingly, GMD derivatives with improved properties covering 17-AAG, 17-DMAG and IPI-504 have been evaluated in clinical trials[21–23]. Radicicol derived and purine related Hsp90 inhibitors currently enter the different stages of clinical trials[24]. Due to several limitations such as: poor solubility, hepatotoxicity, limited metabolic stability and dose-limiting side effects in animals, it is necessary to make efforts to design more potent and safer inhibitors of Hsp90[20, 22].

The discovery of novel compounds as starting point for majorization remains a main challenge. Fragment-based drug discovery (FBDD) presented by Jencks[25] in 1981 for the first time has been developed as an efficient technology to discover novel compounds. It combines advantages of random screening with structure-based drug discovery (SBDD). For examples, FBDD requires less fragments for exploring more chemical spaces and can discover promising compounds with great affinity and druggability with higher opportunities[25–26]. First, we can discover active fragments through random screening of built fragment library. Secondly, we acquire some promising compounds through growth, jointing and self-assembly of active fragments. Finally, we will acquire novel-lead compounds through several rounds of crystal structure-directed majorization. To develop HSP inhibitors with fragment-based drug discovery approach, we build a focused fragment library that based on the reported scaffold of HSP90 inhibitors. Among them, FS36 was designed according to the 2, 4-dihydroxybenzamide moiety, which is a common scaffold found in clinical trail drugs, such as AUY-922, AT13387[27–28].

Here, a novel human Hsp90 inhibitor FS36 has been designed by FBDD and synthesized. Furthermore, the complex crystals of FS36 and Hsp90^N were grown and a high-resolution crystal structure was determined by XRD, which has been deposited in PDB (PDB code 4L93). The crystal structure of Hsp90^N-FS36 was analyzed in detail and compared with the crystal structure of Hsp90^N and ATP-Hsp90^N respectively. The complex crystal structure and the interaction between FS36 and Hsp90^N lay a rational foundation of the design and majorization of novel anticancer drugs targeting Hsp90^N with better quality.

2　Experimental section

2.1　Synthesis of the small molecule FS36

As shown in Figure 1, compound *1* reacted with bromine in alkaline condition to give compound *2*, followed by condensation with 1,2,3,4-tetrahydroisoquinoline to get compound *3*, which deprotected by boron trichloride to yield the target compound b.

2.2　Protein purification and crystallization

The cloned recombinant plasmid including the gene of human Hsp90α N-terminal domain (residues 9–236) and pET28a vector was transformed into *E. coli* Rosetta (DE3) pLysS in order to over-express target Hsp90^N (Invitrogen, Carlsbad, America). The bacteria were grown in 800 ml Luria-Bertani (LB) broth at 37℃ to an A_{600} value reaching 0.6–0.8 and subsequently induced by 200 μmol/L isopropyl β-D-thiogalactopyranoside (IPTG) for 3–5 h at 30℃. The over-expressed bacteria were gathered *via*
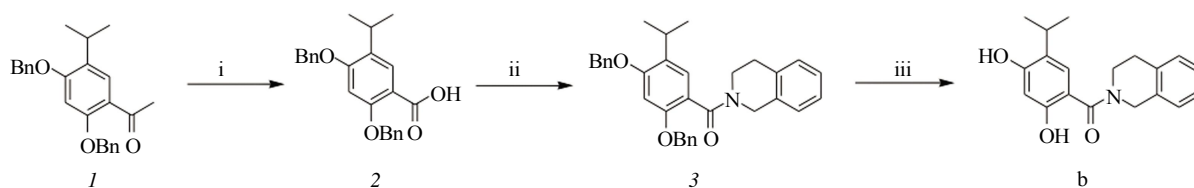
Fig. 1　Synthesis of compound FS36 b

(i) Br$_2$, 1N NaOH solution, dioxane, H$_2$O, 0℃, 4 h, 45%. (ii) 1, 2, 3, 4-Tetrahydroisoquinoline, 1-Hydroxybenzotriazole, N-(3-Dimethylaminopropyl)-N'-ethylcarbodiimide hydrochloride, N, N-Diisopropylethylamine, DMF, rt. 12 h, 76%. (iii) BCl$_3$, DCM, 0℃, 2 h, 63%.

centrifugation at 10 000 g for 10 min (CF16RX, Hitachi, Japan). The sediment was re-suspended in buffer A (pH 7.5, 0.1 mol/L Tris-HCl, 0.3 mol/L NaCl and 5% glycerol) and subsequently smashed by ultra-high pressure cell disrupter (JN-02C, JNBIO, China). The above product was centrifuged at 30 000 g for 30 min at 4℃ for preliminary purification and the supernatant was loaded onto a 5 ml Ni^{2+}-nitrilotriacetate column (Ni-NTA, GE Healthcare, America). The interest protein was eluted with buffer B (pH 7.5, 0.1 mol/L Tris-HCl, 0.3 mol/L NaCl, 0.1 mol/L imidazole and 5% glycerol). The depurated protein was concentrated and the buffer was replaced with buffer C (pH 7.5, 0.1 mol/L Tris-HCl, 0.15 mol/L NaCl and 10% glycerol) using a 10 000 Mr cut-off centrifugal concentrator (Amicon Ultra-15, Millipore, America). The impurities were got rid of by a gel filtration column (Superdex 75 PG, GE Healthcare, America) with buffer C in order for fine purification. The depurated protein was analyzed by a 15% SDS-PAGE to determine the purity. The fine depurated protein was concentrated to a concentration of approximately 20 g/L with the 10 000 Mr cut-off centrifugal concentrator again and its concentration was determined via bicinchoninic acid method (BCA). The fine depurated Hsp90^N was flash-frozen in liquid nitrogen and stored at –80℃.

The concentration of Hsp90^N was about 20 g/L in order for crystallization. The small molecular inhibitor FS36 was added to Hsp90^N according to a 3 : 1 molar ratio and the mixture was incubated for 30 min on ice. We adopted the hanging drop vapor diffusion method in an incubator controlled by a bath circulator (PolyScience 9712, PolyScience, USA) to conduct the co-crystallization in the condition of 4℃ for 2–3 days. The co-crystals were grown under the condition which had a little difference from native crystal[9]: pH 6.5, 0.2 mol/L magnesium chloride, 0.1 mol/L sodium cacodylate, 20%–25%(w/v) polyethylene glycol 2 000 monomethyl ether (PEG2000 MME).

2.3　Data collection, structure determination and refinement

Co-crystals were mounted with cryo-loop (Hampton research, America) and flash-frozen in liquid nitrogen for data collection. All data sets were collected at 100 K on Macromolecular Crystallography Beamline17U1 (BL17U1) at Shanghai Synchrotron Radiation Facility (SSRF, Shanghai, China) by means of an ADSC Quantum 315r CCD detector[29]. We used the HKL 2000 software package to integrate and merge all data. The molecular replacement using PHENIX software determined the structures[30]. The research mode for the crystal is the structure of Hsp90^N which is previously reported (PDB code 3T0H)[9]. The initial model was rebuilt by the program Coot[31]. We used the PHENIX software to refine the model whose resolution limit reached 1.85Å and analyzed the contrast of the overlay with PyMOL package[32].

3　Results and discussion

3.1　Purification, crystallization and structure determination of Hsp90^N-FS36

Hsp90^N was purified to obvious homogeneity by means of metal chelating chromatography, followed by gel filtration chromatography. The single elution volume peak was in accord with monomeric Hsp90^N with a molecular mass of 25 ku and showed a good purity which was assessed by SDS-PAGE, as shown in Figure 2 (the purity of protein reach 98%). We used the hanging-drop method to obtain the crystals of Hsp90^N-FS36 complex at 277 K. The crystals of complex were grown about the dimension of 200 μm×100 μm×50 μm, as shown in Figure 3.
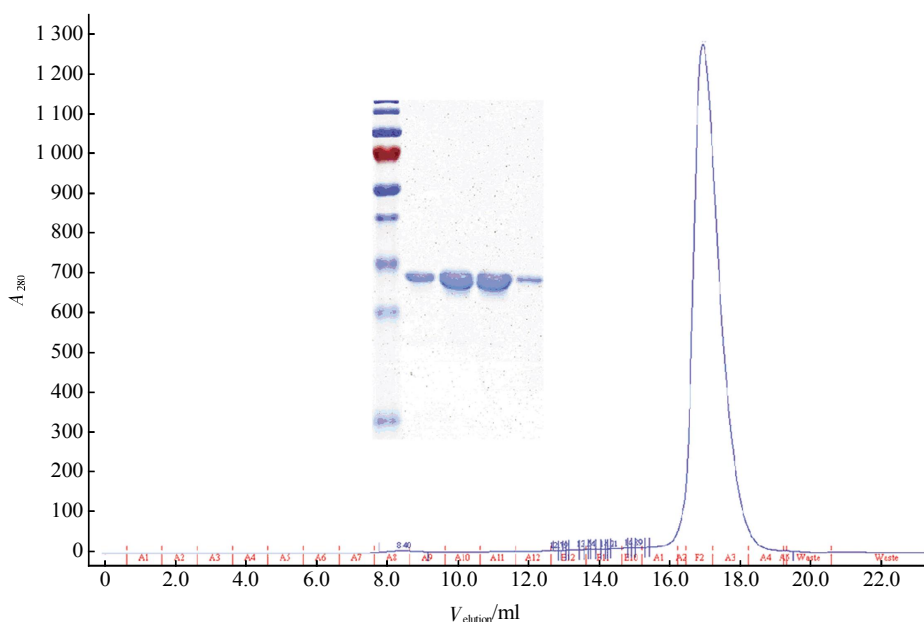
Fig. 2 Purification of Hsp90^N

Size-exclusion chromatography and SDS-PAGE analysis of purified Hsp90^N. A single peak was observed for the purified protein solution.
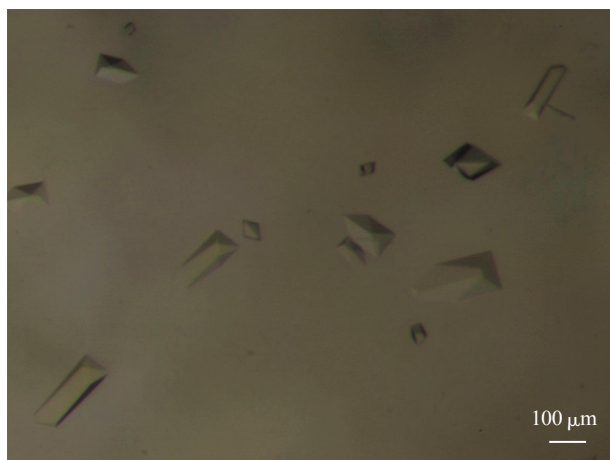
Fig. 3 The crystals of the Hsp90^N-FS36 complex obtained by the hanging-drop method at 277 K

The average dimension of the crystals was about 200 μm×100 μm×50 μm.

We used the structure of Hsp90^N which is previously reported (PDB code 3T0H)[9] as the research mode to determine the structure of Hsp90^N-FS36 which have been deposited in PDB (PDB code 4L93) by molecular replacement. The statistics for data processing and model refinement of Hsp90-FS36 complexes are revealed in Table 1. The diffraction data were collected to 1.85Å resolution and indexed in space groups: I222. The unit cell parameters were: $a = 64.32$Å, $b = 88.83$Å, $c = 98.18$Å; $\alpha = \beta = \gamma = 90.00$Å. The refined model includes residues: Val17-Lys224

and no electron density was observed for residues: Asp9-Glu16 and Glu225-Glu236 in the structure. The missing residues which exist at the N- and C-termini of the model and they are possible to be disordered.

Table 1 Statistics for data processing and model refinement of Hsp90-FS36 complexes

PDB code	4L93
Synchrotron	SSRF
Beam line	BL17U1
Wavelength/Å	0.97915
Space group	I222
a, b, c/Å	64.32, 88.83, 98.18
α, β, γ /°	90.00，90.00，90.00
Resolution/Å	1.85 (1.88–1.85)
R-merge/%	6.4 (52.7)
I / σ (I)	30.1 (3.1)
Completeness/%	99.7 (99.9)
Redundancy	4.1 (3.9)
Resolution/Å	30.56–1.85
R_{work} (R_{free})	0.223 (0.26)
Mean temperature factor/Å^2	31.2
Bond lengths/Å	0.006
Bond angles/°	1.02
Favored	94.63
Allowwed	4.63
Outliers	0.73

Values in parentheses are for the highest-resolution shell.

3.2 Analysis of crystal structure and interaction of Hsp90ᴺ-FS36

From the complex crystal structure, we can find FS36 was bound to the ATP-binding pocket of Hsp90 completely and its integrated electron density has been captured, as shown in Figure 4.

We can find the electrostatic potential surface surrounding the active site of Hsp90ᴺ-FS36 and Hsp90ᴺ-ATP shown in Figure 5. The changes compared with Hsp90ᴺ happened in electrostatic potential surface surrounding the active pocket of Hsp90ᴺ used for binding ATP, FS36 and other small molecules. The active site of Hsp90 binding ATP has in common with binding FS36 and they are both located in the ATP binding site. Interestingly, the binding of FS36 induces the conformational rearrangements of L6 and leaves a larger room for conformational modification of FS36 further because of the longer and wider ATP binding pocket.
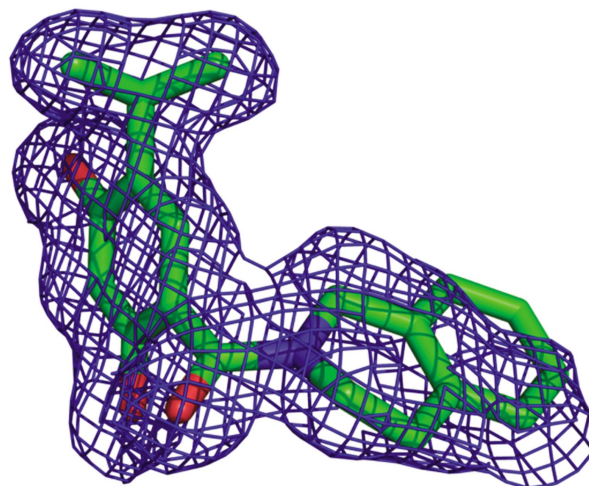
Fig. 4 Electron density map (2Fo-Fc) of FS36

The map was contoured at 1∶0σ and the stick is used to represent the refined FS36 model. Carbon, nitrogen and oxygen atoms are shown green, blue and red, respectively.
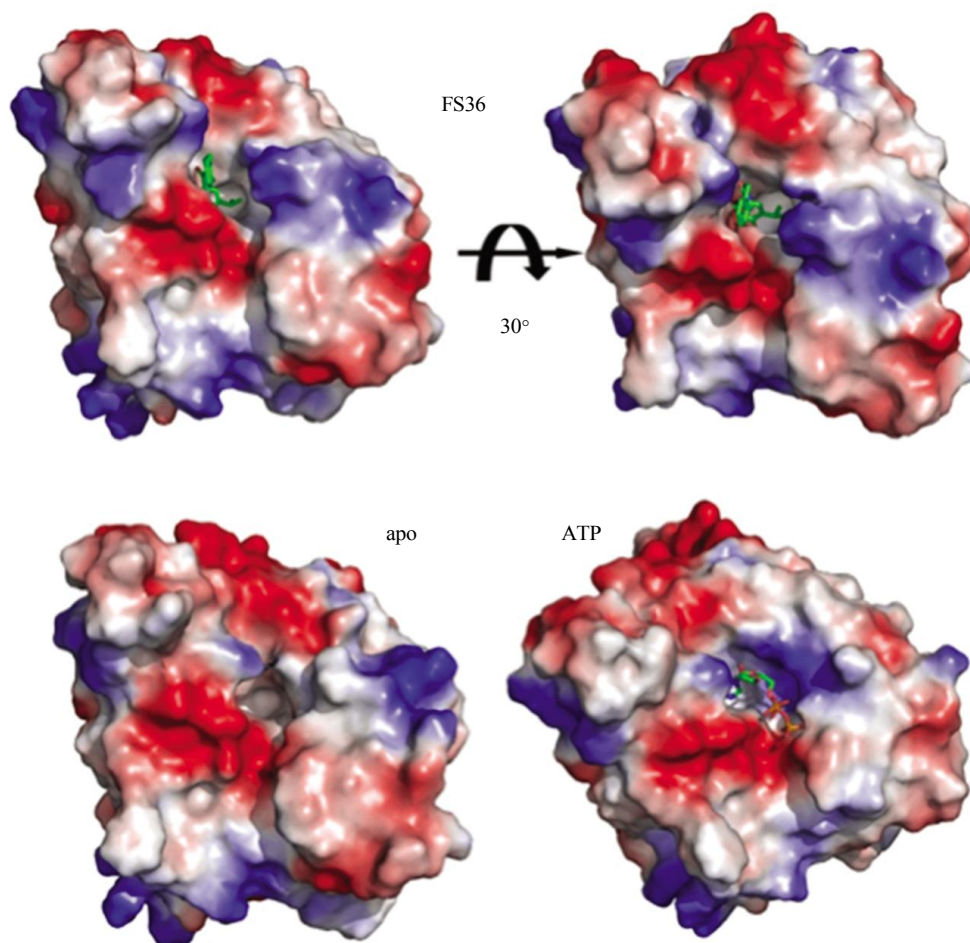
Fig. 5 Electrostatic potential surface distribution of Hsp90ᴺ and the binding of FS36 as well as ATP

We obtained the electrostatic potential by the crystal complexes surface colored, red for negative charge, blue for positive charge, FS36 and ATP in stick representation.

Just as the reported Hsp90^N-ATP complex structure [10], the structural rearrangement of ATP lid composed of H1, H4, H5, and L6 is also shown in Hsp90^N-FS36 complex structure in Figure 6. The ATP lid has two different structures: open or close which is responsible for adjusting the size and accessibility of pocket [12]. The diameter near the entrance of pocket reaches approximately 12Å. H4 and H5 helixes of pocket undergo helix-to-coil and coil-to-helix transitions that propel the structural rearrangement of

L6 including rolling-over 180° and moving toward the pocket to replace portion of H4 helix as one of the pocket walls when binding the small molecular FS36. Thus, the L6 loop plays an important role in constricting the pocket entrance and helping the pocket turn into closed conformation which leads to the failure of ATP-binding and chaperone function. The misfolding and immature client proteins are then hydrolyzed by the proteasomes. Therefore, FS36 can act as a promising inhibitor against cancer.
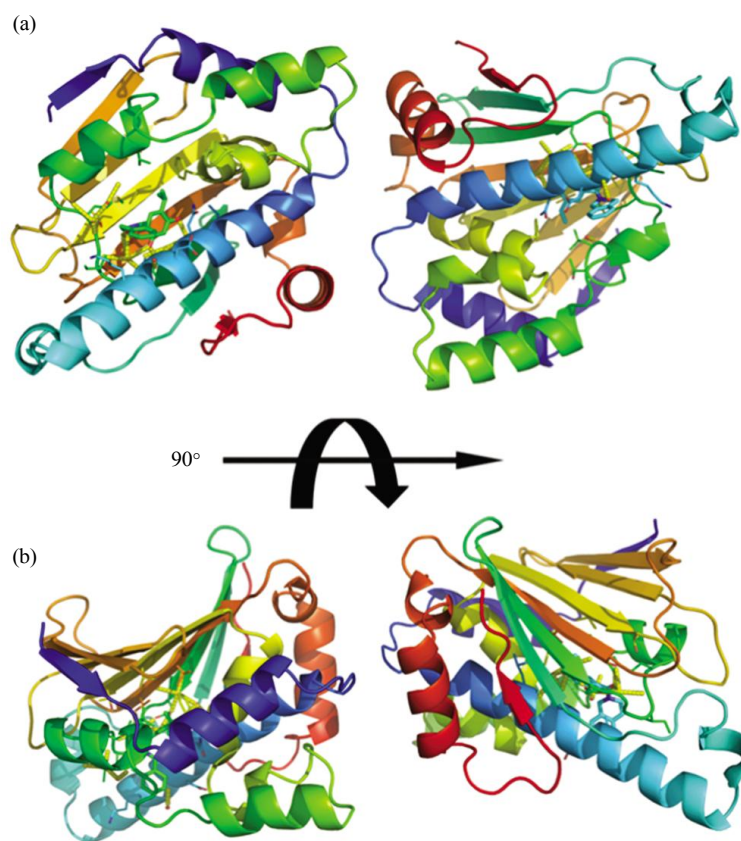
Fig. 6　The structural rearrangement of ATP lid in binding FS36
(a) ATP lid is in the open state under normal condition. (b) When binding the small molecular FS36, ATP lid turns into the closed state.

There are two hydroxyls in the benzene of FS36 shown in Figure 7b. Two water-mediated hydrogen bonds are formed by the 4-hydroxyl close to the isopropyl with residue Ser52 and Leu48. The 2-hydroxyl forms a direct hydrogen bond with residue Asp93 and three water-mediated hydrogen bonds with residue Asp93, Thr184 and Ile96, respectively. The carbonyl of FS36 forms a direct hydrogen bond with residue Thr184 and three water-mediated hydrogen

bonds with residue Asp93, Ile96 and Thr184, respectively. The direct hydrogen bonds and water-mediated hydrogen bonds are crucial for maintaining fine affinity between FS36 and Hsp90^N. Besides, extensive surface complementarity between FS36 and the pocket leading to a high density of van der Waals contacts also makes the binding of FS36 and Hsp90^N more firmly.
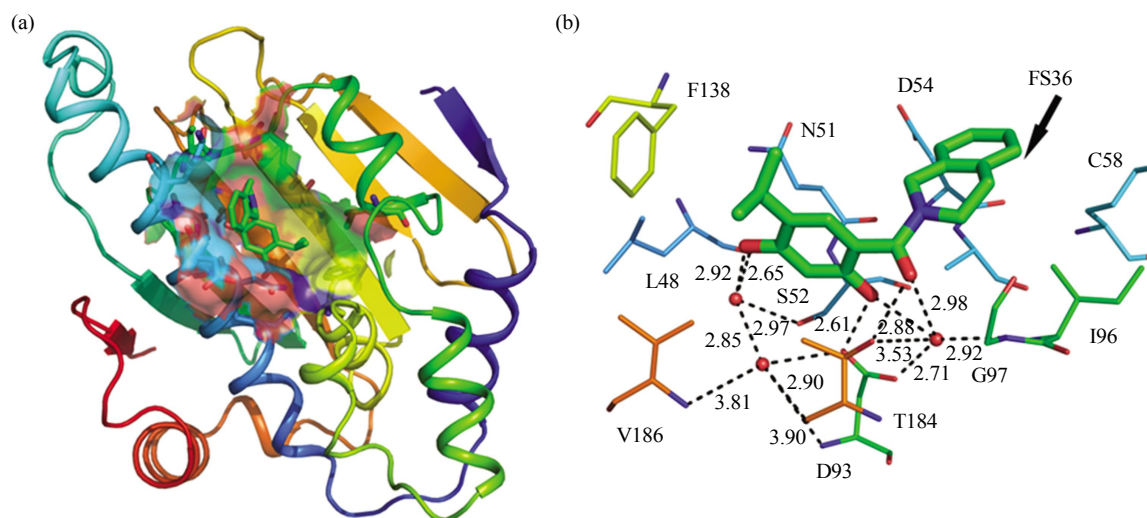
Fig. 7 The interactions between Hsp90ᴺ and FS36

(a) Surface representation of FS36 bound in the pocket of Hsp90ᴺ, FS36and Hsp90 represented in stick and cartoon, respectively. (b) Interactions between FS36 and Hsp90ᴺ. Carbon, nitrogen and oxygen atoms in FS36 are shown green, blue and red, respectively. Water molecules are represented by red spheres and black dashed lines with the distance between two atoms labeled represent hydrogen bonds.

4 Conclusion

Hsp90ᴺ is proved to be a highly conserved pocket where residues are necessary for chaperone functions. A novel anti-cancer inhibitor FS36 has been designed by means of and synthesized to interact with these residues of pocket. The Hsp90ᴺ-FS36 crystal structure was deposited in PDB (code 4L93). From the complex crystal structure, we have reasons to believe FS36 was bound to the ATP-binding pocket of Hsp90 completely. The structural rearrangement of L6 plays an important role in leading to the failure of ATP-binding and chaperone function. Then, L6 possesses a larger room for conformational modification of FS36 further. Thus, the progression of cancer such as appropriate folding, conformational maturation can be blocked effectively and FS36 can act as a potent anti-cancer lead compound. Meanwhile, the crystal structure of FS36-Hsp90ᴺ shows a detailed mechanism of interaction and lays the foundation for the design of more potent and safer small inhibitors.

References

[1] Ren J, Yang M, Liu H, *et al*. Multi-substituted 8-aminoimidazo [1,2-a]pyrazines by groebke-blackburn-bienaymé reaction and their Hsp90 inhibitory activity. Org Biomol Chem, 2015, **13**(5): 1531– 1535

[2] Cao H L, Sun L H, Liu L, *et al*. Structural consistency analysis of recombinant and wild-type human serum albumin. J Mol Struct, 2017, **1127**: 1–5

[3] Li J, Shi F, Chen D Q, *et al*. FS23 binds to the N-terminal domain of human Hsp90: a novel small inhibitor for Hsp90. J Nucl Sci Tech, 2015, **26**(6): 108–114

[4] Mayer M P, Le Breton L. Hsp90: breaking the symmetry. Mol Cell, 2015, **58**(1): 8–20

[5] Prodromou C, Roe S M, O' Brien R, *et al*. Identification and structural characterization of the ATP/ADP binding site in the Hsp90 molecular chaperone. Cell, 1997, **90**(1): 65–75

[6] Harris S F, Shiau A K, Agard D A. The crystal structure of the carboxy-terminal dimerization domain of htpG, the *Escherichia coli* Hsp90, reveals a potential substrate binding site. Structure, 2004, **12**(6): 1087–1097

[7] Stebbins C E, Russo A A, Schneider C, *et al*. Crystal structure of an Hsp90–geldanamycin complex: targeting of a protein chaperone by an antitumor agent. Cell, 1997, **89**(2): 239–250

[8] Prodromou C, Panaretou B, Chohan S, *et al*. The ATPase cycle of Hsp90 drives a molecular 'clamp' *via* transient dimerization of the N-terminal domains. EMBO J, 2000, **19**(16): 4383–4392

[9] Li J, Sun L, Xu C, *et al*. Structure insights into mechanisms of ATP hydrolysis and the activation of human heat-shock protein90. Acta Biochim Biophys Sin, 2012, **44**(4): 300–306

[10] Murray C W, Verdonk M L, Rees D C. Experiences in fragment-based drug discovery. Trends Pharmacol Sci, **33** (5): 224–232

[11] Stebbins C E, Russo A A, Schneider C, *et al*. Crystal structure of an Hsp90-geldanamycin complex: targeting of a protein chaperone by an antitumor agent. Cell, 1997, **89**(2): 239−250

[12] Sung N, Lee J, Kim J H, *et al*. Mitochondrial Hsp90 is a ligand-activated molecular chaperone coupling ATP binding to dimer closure through a coiled-coil intermediate. Proc Natl Acad Sci USA, 2016, **113**(11): 2952−2957

[13] Hartl F U, Bracher A, Hayer-Hartl M. Molecular chaperones in protein folding and proteostasis. Nature, 2011, **475**(7356): 324−332

[14] Saibil H. Chaperone machines for protein folding, unfolding and disaggregation. Nat Rev Mol Cell Biol, 2013, **14**(10): 630−642

[15] Paul S, Mahanta S. Association of heat-shock proteins in various neurodegenerative disorders: is it a master key to open the therapeutic door? Mol Cell Biochem, 2014, **386**(1−2): 45−61

[16] Hong DS, Banerji U, Tavana B, *et al*. Targeting the molecular chaperone heat shock protein 90 (Hsp90): lessons learned and future directions. Cancer Treat Rev, 2013, **39**(4): 375−387

[17] Schopf F H, Biebl M M, Buchner J. The Hsp90 chaperone machinery. Nat Rev Mol Cell Biol, 2017, **18**(6): 345−360

[18] Wang Y, Jin F, Wang R, *et al*. Hsp90: a promising broad spectrum antiviral drug target. Arch Virol, 2017, **162**(11): 3269−3282

[19] Shiau A K, Harris S F, Southworth D R, *et al*. Structural analysis of *E. coli* Hsp90 reveals dramatic nucleotide-dependent conformational rearrangements. Cell, 2006, **127**(2): 329−340

[20] Jego G, Hazoumé A, Seigneuric R, *et al*. Targeting heat shock proteins in cancer. Cancer Lett, 2013, **332**(2): 275−285

[21] Banerji U, O'Donnell A, Scurr M, *et al*. Phase Ⅰ pharmacokinetic and pharmacodynamic study of 17-allylamino 17-demethoxygeldanamycin in patients with advanced malignancies. J Clin Oncol, 2005, **23**(18): 4152−4161

[22] Jhaveri K, Taldone T, Modi S, *et al*. Advances in the clinical development of heat shock protein 90 (Hsp90) inhibitors in cancers.

[23] Hanson B E, Vesole D H. Retaspimycin hydrochloride (IPI-504): a novel heat shock protein inhibitor as an anticancer agent. Expert Opin Investig Drugs, 2009, **18**(9): 1375−1383

[24] Chatterjee S, Burns T F. Targeting heat shock proteins in cancer: a promising therapeutic approach. Int J Mol Sci, 2017, **18**(9). pii: E1978

[25] Jencks W P. On the attribution and additivity of binding energies. Proc Natl Acad Sci USA, 1981, **78**(7): 4046−4050

[26] Murray C W, Verdonk M L, Rees D C. Experiences in fragment-based drug discovery. Trends Pharmacol Sci, 2012, **33**(5): 224−232

[27] Dunna N R, Bandaru S, Akare U R, *et al*. Multiclass comparative virtual screening to identify novel Hsp90 inhibitors: a therapeutic breast cancer drug target. Curr Top Med Chem, 2015, **15**(1): 57−64

[28] Woodhead A J, Angove H, Carr M G, *et al*. Discovery of (2,4-Dihydroxy-5-isopropylphenyl) - [5- (4-methy lpiperazin-1-ylmethyl)-1,3-dihydroisoindol-2-yl]methanone (AT13387), a novel inhibitor of the molecular chaperone Hsp90 by fragment based drug design. J Med Chem, 2010, **53**(16): 5956−5969

[29] Wang Q S, Yu F, Huang S, *et al*. The macromolecular crystallography beamline of SSRF. Nucl Sci Tech, 2015, **26**: 010102

[30] Adams P D, Afonine P V, Bunkóczi G, *et al*. PHENIX: a comprehensive Python-based system for macromolecular structure solution. Acta Crystallogr D Biol Crystallogr, 2010, **66** (Pt 2): 213−221

[31] Emsley P, Cowtan K. Coot: Model-building tools for molecular graphics. Acta Crystallogr D Biol Crystallogr, 2004, **60**(Pt 12 Pt 1): 2126−2132

[32] Grell L, Parkin C, Slatest L, *et al*. A tool for simplifying molecular viewing inPyMOL. Biochem Mol Biol Educ, 2006, **34**(6): 402−407

Biochim Biophys Acta, 2012, **1823**(3): 742−755

FS36 作为新型人源 Hsp90 抑制剂的发现 *

李　根 [1)]　吕凯凯 [2)]　李　健 [1, 3)]　尹秀山 [1, 4)]　赵　栋 [5)]　张万忠 [1)**]

([1)] 沈阳化工大学制药与生物工程学院，沈阳 110142；[2)] 中国科学院上海药物研究所，上海 201203；

[3)] *Department of Molecular & Cellular Biochemistry, College of Medicine, University of Kentucky, Lexington, KY 40536, USA;*

[4)] *Karolinska Institutet (MTC), Science for Life Laboratory, Tomtebodavãg, en 23A (Gamma5), 17165 Solna, Sweden;*

[5)] 西安医学院基础与转化医学研究所，西安 710021)

摘要 热休克蛋白 90(Hsp90)通过对几百种蛋白质底物(客户蛋白质)进行合理的折叠、成熟其构象并且激活，在肿瘤细胞的生长和繁殖中发挥重要作用. 因此，Hsp90 成为非常有吸引力、有前途的抗肿瘤药物靶点，并且超过 20 种抑制剂已经进入临床实验阶段. 我们在这里设计并合成了一个小分子抑制剂：FS36. 收集了 Hsp90^N-FS36 复合物晶体结构的 X 射线衍射实验数据. 高分辨率 X 射线晶体结构表明，FS36 在 ATP 结合位点上与 Hsp90^N 相互作用，并且 FS36 可能替代核苷酸与 Hsp90^N 结合. FS36 和 Hsp90^N 的复合物晶体结构和相互作用为后期设计和优化新型抗肿瘤药物奠定基础.

关键词 热休克蛋白 90，抗肿瘤药物，抑制剂，X 射线衍射，复合物晶体结构
学科分类号 R91，Q617 　　　　　　　　　　　**DOI**: 10.16476/j.pibb.2017.0451